Environ. Sci. Technol. **2003**, *37,* 529−534

Nickel Sequestration in a Kaolinite-Humic Acid Complex

MAARTEN NACHTEGAAL* AND DONALD L. SPARKS

Department of Plant and Soil Sciences, University of Delaware, 152 Townsend Hall, Newark, Delaware 19717-1303

Incorporation of first row transition metals into stable surface precipitates can play an important role in reducing the bioavailability of these metals in neutral and alkaline soils. Organic coatings may interfere with this sorption mechanism by changing the surface characteristics and by masking the mineral surface from metal sorptives. In this study, kinetic sorption and desorption experiments were combined with extended X-ray absorption fine structure (EXAFS) spectroscopy to elucidate the effect of humic acid (HA) coatings on the formation and stabilization of nickel precipitates at the kaolinite−water interface. Initial Ni uptake (pH 7.5, $[Ni]_i = 3$ mM, and $I = 0.02$ M $NaNO_3$) increased with greater amounts of HA coated onto the kaolinite surface. Ni uptake continued over an extended period of time without reaching an apparent equilibrium. EXAFS analysis of the Ni sorption complex structures formed over time (up to 7 months) revealed the formation of a Ni−Al layered double hydroxide (LDH) precipitate at the kaolinite surface in the absence of HA. HA alone formed an inner-sphere complex with Ni (with 2 carbon atoms at an average radial distance of 2.85 Å). A Ni−Al LDH precipitate phase was formed at the kaolinite surface in the presence of a 1 wt % HA coating. However, with 5 wt % HA coated at the kaolinite surface, the formation of a surface precipitate was slowed significantly, and the precipitate formed was similar in structure to $Ni(OH)_2$(s). The $Ni(OH)_2$ precipitate was not resistant to proton dissolution, while the Ni−Al LDH precipitate was. These results augment earlier findings that the incorporation of Ni and other first row transition metals into stable surface precipitates is an important sequestration pathway for toxic metals in the environment, despite the presence of ubiquitous coating materials such as humic acids.

Introduction

The mobility and bioavailability of trace metals in soils is largely dictated by reactions taking place at the soil solution−particle interfaces (*1, 2*). Therefore, a complete understanding of long-term metal availability depends on knowing the adsorption and desorption reactions taking place at the soil particle surfaces. Laboratory studies of metal partitioning identified the incorporation of Cr, Ni, Co, Cu, and Zn into a neoformed surface precipitate as the primary sorption mechanism for these potentially toxic metals at pH > 6.0 (*3*−*10*). Depending on the reaction conditions, time, and absorbent phase present, either a metal hydroxide, a mixed layered double hydroxide (LDH), or a phyllosilicate formed at the mineral surfaces (*11*−*15*). These neo-formed phases form well below theoretical monolayer coverage and in a pH range at which metal hydroxide precipitates would not be expected to form according to their thermodynamic solubility product. The precipitates are stabilized upon aging (*14, 16*). This stabilization has been attributed to the transformation of a mixed layered double hydroxide phase into a more stable phyllosilicate phase and/or to Ostwald ripening. Identification of the potential of surface precipitate formation in nonacidic soils is important since this sorption process might lead to the long-term removal of potentially hazardous first row transition metals from the soil solution.

Zn-containing surface precipitates have recently been identified in soils close to smelter facilities (*17, 18*). The conditions in these soils are favorable for the formation of precipitates, with high concentrations of metal (weight percent) present, alkaline pH, and relatively small amounts of organic matter. Organic matter and particularly humic substances (HS), the stable organic pool in soils, can strongly compete for metal uptake with the mineral surface and may mask the mineral surface from metals in the solution phase (*19*−*21*). Humic substances are ubiquitous in soils and are often intimately associated with clay minerals (*19*). A study on Ni sorption mechanisms on the clay fraction of a Matapeake silt loam, with and without a small organic fraction (∼1 wt %) present, suggested that Ni−Al layered double hydroxides formed in soils with low organic matter content (*22*). However, identification of Ni sorption complexes that have formed in whole soils is challenging because of the limitations of current available spectroscopic techniques in separating a broad array of sorption sites, each with a unique spectroscopic signature.

Our understanding of the relative importance of surface precipitate formation in natural systems can be improved by examining the effect of individual competitive sorbents on the mechanism of surface precipitate formation. Elzinga and Sparks (*23*) studied the competition between Ni adsorption onto montmorillonite and Ni surface precipitate formation on pyrophyllite and found that neither mechanism was dominating. Yamaguchi et al. (*24*) studied the influence of small organic acids, i.e., citrate and salicylate, on Ni sorption onto gibbsite and pyrophyllite. These organic acids suppressed Ni removal from solution and the formation of a surface precipitate. These results were attributed to strong metal complexation by the small organic acids in solution. Conversely, a study by Zachara et al. (*25*) on Co^{2+} sorption by a subsurface mineral separate showed that the presence of a humic acid coating augmented rather than changed the intrinsic sorption behavior of the mineral sorbents. This suggests that humic substances, especially when coated onto mineral surfaces, may have a different effect on Ni uptake behavior than do small organic molecules in solution.

In the present study, macroscopic Ni sorption and desorption kinetic studies are combined with extended X-ray absorption fine structure (EXAFS) spectroscopy to characterize the structure and stability of the sorption complex formed on kaolinite coated with humic acid (HA). The objective of the present work is to elucidate the effects of HA coatings on mechanisms of Ni surface precipitate formation and stabilization. A range of organic matter contents representative of those found in soils is used as coatings (*2*). The HA coatings may interfere with the intrinsic Ni sorption mechanisms to kaolinite in several ways: First of all, formation of Ni and Al organic complexes can reduce the availability of these metals for the formation of a precipitate phase. On the contrary, enhanced mineral dissolution by organic acids can lead to

* Corresponding author phone: (302)831-1595; fax: (302)831-0605; e-mail: maarten@udel.edu.

10.1021/es025803w CCC: $25.00
Published on Web 12/18/2002

TABLE 1. Physicochemical Characteristics of the Solids Used in This Study

	CEC (mequiv 100 g^{-1})[a]	BET surface area (m^2 g^{-1})
kaolinite	9.37 (pH 6.0)	14.01
1 wt % HA-kaolinite	25.80 (pH 5.5)	13.42
5 wt % HA-kaolinite	29.62 (pH 5.5)	11.68
humic acid	83.83 (pH 3.6)	1.25

[a] CEC, cation exchange capacity, determined by Ba−Mg exchange, unbuffered.

a larger availability of Al and Si for the stabilization of the precipitate. Second of all, the metal uptake capacity of the coated kaolinite is significantly higher than that of kaolinite because of the larger surface area and cation exchange capacity (CEC) of the HA-coated kaolinite. Additionally, the presence of organic coatings may alter the reactivity of the underlying kaolinite surface by forming inner-sphere complexes with the highly reactive aluminol groups of the kaolinite edge sites and by modifying the electrical properties of the kaolinite−water interface (*26*).

Materials and Methods

Materials. The kaolinite used in this study is a well-crystallized Georgia kaolinite, Clay Mineral Society source clay (KGa-1). The kaolinite was treated for the possible presence of carbonates, organic matter, and manganese/iron oxides using standard procedures (*27*). Carbonates and exchangeable divalent ions were removed by reaction with a NaOAc buffer at pH 5 in a near boiling warm water bath. Organic matter was removed by treatment of the kaolinite with 30% H_2O_2. Iron oxides were removed with a dithionite−citrate−bicarbonate mixture in a 80 °C warm water bath. The resulting kaolinite was washed twice with a 1.0 M NaCl solution and twice with DI water. The <0.2-μm fraction was separated by centrifugation, dialyzed against Milli-Q H_2O, and freeze-dried.

A well-characterized HA (*28*) isolated from a bog-soil collected in the White Mountain National Forest in Rumney, NH, was supplied by Drs. G. Davies and E. A. Ghabbour (Northeastern University, Boston, MA). The isolation procedure and characterization of the HA are outlined elsewhere (*28*). Essentially the soil was pretreated with mild solvents (a benzene−methanol mixture). After being pre-extracted, the humic substances were extracted with aqueous base. The ash content of this HA is 0.25 wt %. The supernatant was brought to pH 1.0 with concentrated HCl. The remaining HA gel was washed and freeze-dried before any further use.

Humic acid-coated kaolinite samples containing 1 and 5 wt % of humic acid were prepared by dissolving 0.01 g (1 wt %) and 0.05 g (5 wt %) of HA in 50 mL of a N_2-purged 0.05 M NaOH solution. The HA solution was brought to pH 7.5 prior to mixing with 1 g of kaolinite. The pH of the kaolinite−humic acid suspension was brought to 3.5. This mixture was shaken for 48 h and brought to 200 mL, pH 7.5, and $I = 0.02$ M $NaNO_3$ prior to the sorption experiments. For all experiments, the mass of kaolinite was maintained constant (5 g L^{-1}) while the fraction of organic matter was varied. The cation exchange capacity (CEC) of the solids was determined by Ba−Mg exchange, without pH buffering. The specific surface area of the solids was determined by a five-point N_2 Brunauer−Emmett−Teller (BET) gas adsorption isotherm method. The CEC and the specific surface area of the mixtures and individual components are given in Table 1.

Nickel Sorption Experiments. The kinetics of Ni partitioning to kaolinite (hydrated in the background solution for 48 h), 5 wt % HA (dissolved in 0.05 M NaOH, precipitated at pH 3.0, after which the pH was raised to pH 7.5), and kaolinite coated with 1 and 5 wt % HA were studied in batch reactors. Experiments were carried out in a 0.02 M $NaNO_3$ background solution and at pH 7.5 since previous research (*4*, *15*) indicated that Ni−Al precipitates do form at this pH in the absence of competing sorbent surfaces. The systems were purged with N_2, and Milli-Q H_2O was used throughout to minimize the formation of carbonates. Nickel from a 0.1 M $Ni(NO_3)_2$ stock solution was added in 1-mL aliquots to achieve an initial [Ni] of 3 mM. The solution was undersaturated with respect to homogeneous precipitation of $Ni(OH)_2$ (*29*). The pH was kept constant at 7.5 using a Radiometer pH-stat titrator (Westlake, OH) for the first 2 days and afterward by weekly manual readjustments using 0.1 M NaOH. Samples (10 mL) were periodically collected from the suspension and filtered through a 0.2-μm membrame filter. Filtered supernatants were analyzed for dissolved Ni by inductively coupled plasma optical emission spectroscopy (ICP−OES). Solid samples were collected after 4 days, 2 weeks, 1 month, and 7 months for characterization using XAFS spectroscopy. Solids were isolated under vacuum filtration and transferred to a polyethylene holder. The wet paste was sealed into the holder with 0.0005-in. Kapton polymide tape (CHR Industries, type K-104) to avoid moisture loss during analysis.

Desorption Experiments. The effect of a 5 wt % HA coating on the reversibility of Ni sorption to kaolinite was studied using a replenishment technique. Thirty milliliter aliquots of suspension were separated from the kaolinite and 5 wt % HA−kaolinite sorption experiments after 7 months of reaction. These aliquots were centrifuged at 2500*g* for 10 min. The supernatants were collected for ICP−OES analysis, the remaining solids were resuspended either in the $NaNO_3$ background electrolyte solution used in the sorption experiments (pH 7.5, $I = 0.02$ M $NaNO_3$), in a $CaCl_2$ solution (pH 6.0, $I = 0.01$ M $CaCl_2$), or in a 0.1 M HNO_3 solution (pH 4.0). The solids were resuspended using a Vortex stirrer, shaken for 24 h at 25 °C in a reciprocal shaker, and centrifuged at 2500*g* for 10 min. This replenishment was repeated 14 times.

XAFS Data Collection and Analyses. X-ray absorption spectra were collected at beamline X-11A of the National Synchrotron Light Source (NSLS), Brookhaven National Laboratory. The electron storage ring operated at 2.8 GeV with an average beam current of 180 mA. The monochromator consisted of two parallel Si(111) crystals with an entrance slit of 0.5 mm. Higher order harmonics were suppressed by detuning 25% from the maximum beam intensity. The monochromator position was calibrated by assigning the first inflection point on the K-edge of a nickel metal foil to 8333.0 eV. The spectra were collected in fluorescence mode using an Ar-filled Lytle detector. A 6-μm Co filter and soller slits were placed between the sample and the detector to reduce elastic scattering. The incoming beam was measured with a N_2-filled ion chamber. All spectra were collected at room temperature, and at least three scans were collected per sample to improve the signal-to-noise ratio.

XAFS data reduction was performed using WinXAS 2.1 following standard procedures (*15*, *30*). The χ function was extracted from the raw data by fitting a linear function to the preedge region and a spline function to the postedge region and normalizing the edge jump to unity. The energy axis (eV) was converted to photoelectron wave vector units ($Å^{-1}$) by assigning the origin, E_o, to the first inflection point of the absorption edge. The resulting $\chi(k)$ functions were weighted with k^3 to compensate for the dampening of the XAFS amplitude with increasing k and were Fourier-transformed to obtain radial structure functions (RSF). A Bessel window with a smoothing parameter of 4 was used to suppress artifacts because of the finite Fourier filtering range between $\Delta k = 1.5-13.8$ $Å^{-1}$. The two major peaks below 3.5 $Å^{-1}$ in the Fourier-transformed curves were isolated and backtransformed. An R range of ≈1.07−2.04 $Å^{-1}$ was used for the first peak, and an R range of ≈2.04−3.28 $Å^{-1}$ was used for the

second. These backtransformed peaks were fit in k space. Structural parameters were extracted with fits to the standard EXAFS equation. Ab initio Ni−O and Ni−Ni/Al (or Ni−C for the HA containing samples) scattering paths were generated using the FEFF 7.02 code from the refinement of the structure of lizardite where Ni was substituted for Mg in octahedral positions (*31*). After each of the individual peaks in the Fourier transform spectra were backtransformed and fit, multishell fitting was done in R space over the range of the first two shells (ΔR = 1.07−3.30) using the same parameters. Optimization of the parameters was then performed again, with the E_o shifts constrained to be equal. The amplitude reduction factor, $(S_o)^2$, was fixed at 0.85. A good fit was determined on the basis of the minimum residual error.

Results and Discussion

Solid Characteristics. The physicochemical characteristics of the solids used in this study are collected in Table 1. The CEC was determined by Ba−Mg exchange and without the presence of a pH buffer since these organic pH buffers could potentially interact with HA. The CECs of the (coated) kaolinite samples were all determined at pH ∼5.5. The CEC increases significantly when kaolinite is coated with increasing amounts of HA. The CEC of the HA was determined at a much lower pH of ∼3.6. Most carboxyl groups deprotonate between pH 4 and pH 6. Therefore, the CEC of HA is expected to be much higher at pH 5.5. Cation exchange capacities ranging from 300 to 1400 cmol kg^{-1} have been reported for HA in the literature (*2*).

The BET surface area values reported in Table 1 compare with values reported in the literature (*32, 33*) and are an indication of the small pore size of HA rather then the external surface area. The reason for this is that nitrogen is subject to molecular sieving at 77 K because of activated diffusion in micropores of HA (*33*). The large HA surface area determined by the ethylene glycol monomethyl ether (EGME) method and reported in the literature is a consequence of polar interactions between HA and EGME. No reliable methods are currently available to determine the precise surface area of humic substances, and subsequently, the total surface loadings could not be reported in this study. The decreasing BET surface area with increasing amounts of HA coated at the kaolinite surface indicates that a significant portion of the kaolinite surface is being covered by the HA.

Adsorption Kinetics. The adsorption of Ni as a function of time was investigated on pristine kaolinite and HA and on 1 and 5 wt % HA-coated kaolinite (Figure 1A,B). Only 8% of the initial Ni concentration was retained by the pristine kaolinite surface after 60 h of reaction, while approximately 40% was retained by the HA-only system, indicating that HA has a much higher reactive surface area than kaolinite. After 60 h, the 1 and 5 wt % HA-coated kaolinite retained approximately 18 and 25% of initial Ni concentrations, respectively. Increasing metal sorption with increasing amounts of HA coated on the mineral surface has also been reported for cobalt sorption to organic matter−mineral complexes (*25*).

The 5 wt % HA has a higher sorption capacity then when the same amount of HA is coated at the kaolinite surface. This suggests that a significant amount of the nickel sorption sites on both kaolinite (edge sites) and HA (mainly carboxylic and phenolic functional groups) have become unavailable as a result of the formation of chemical bonds between the kaolinite and the humic acid.

The release of Ni by the HA after about 30 h of reaction may be caused by the partial dissolution of HA at the basic pH employed in this study. The release of Ni is not observed in the HA-coated kaolinite samples. This is due to a stabilization of HA when it is bound to clay minerals (*19, 34*).

Nickel sorption to kaolinite and kaolinite coated with 1 wt % HA is initially fast and is followed by a slow continued

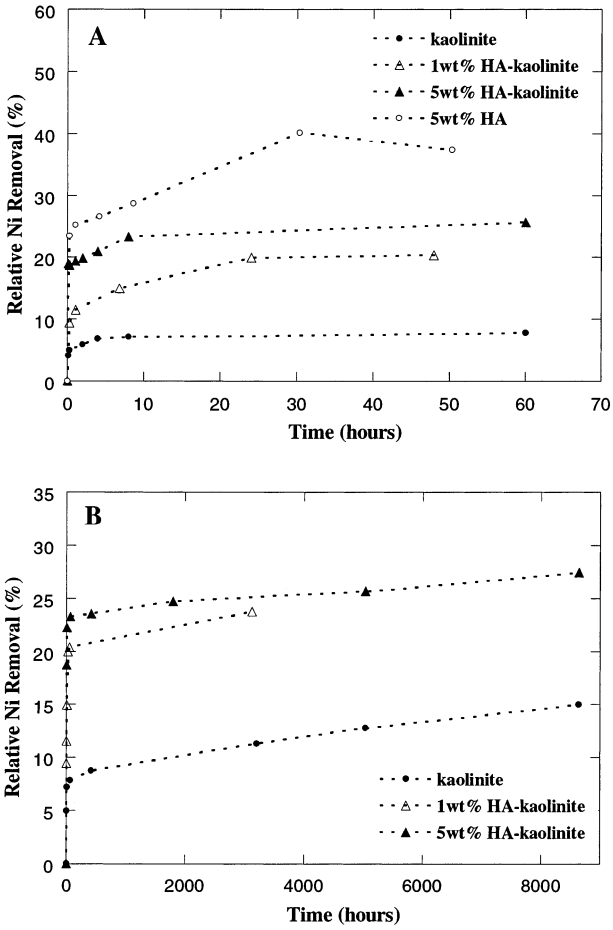

FIGURE 1. Ni sorption kinetics (A) within the first 60 h (initial sorption conditions: pH 7.5, I = 0.02 M $NaNO_3$, $[Ni]_i$ = 3 mM) and (B) Ni sorption kinetics over the entire reaction range.

Ni uptake (Figure 1B). A slow continued Ni uptake can be observed to a lesser extent for the 5 wt % HA−kaolinite. This two-step sorption process is characteristic of heavy metal sorption on clays and oxide surfaces (*4, 35*). Several mechanisms have been proposed for the slow continued metal uptake by clays and oxide surfaces, including adsorption of metals onto sites that have relatively large activation energies (*4, 36, 37*), diffusion into micropores of the minerals (*37, 38*), and a continuous growth of a surface precipitate away from the sorbent surface (*30*). EXAFS studies indicated the formation of Ni−Al LDH at the kaolinite surface under the reaction conditions employed in this study and in the absence of organic matter (*4, 30*). Therefore, it is likely that the growth of a surface precipitate away from the kaolinite surface is responsible for the continued Ni uptake by the kaolinite. Driving forces for a continuous growth of a surface precipitate include the continued presence of Ni in solution and the increase in surface area because of the formation of a precipitate phase. It is likely that several sorption mechanisms are involved in the Ni uptake by the HA-coated kaolinite systems since several different sorption sites are available in these systems. The higher initial Ni sorption in the HA-coated systems and the slower continued Ni uptake (about 12% of the initial Ni sorption in 9000 h) as compared to the pristine kaolinite (almost double the initial Ni sorption) indicate that, besides the formation of a surface precipitate, the formation of sorption complexes with the functional groups of HA play an important role in the sequestration of Ni (see also EXAFS discussion later in this paper).

Desorption Behavior. To compare the stability of the sorption complexes formed at the kaolinite−water and the

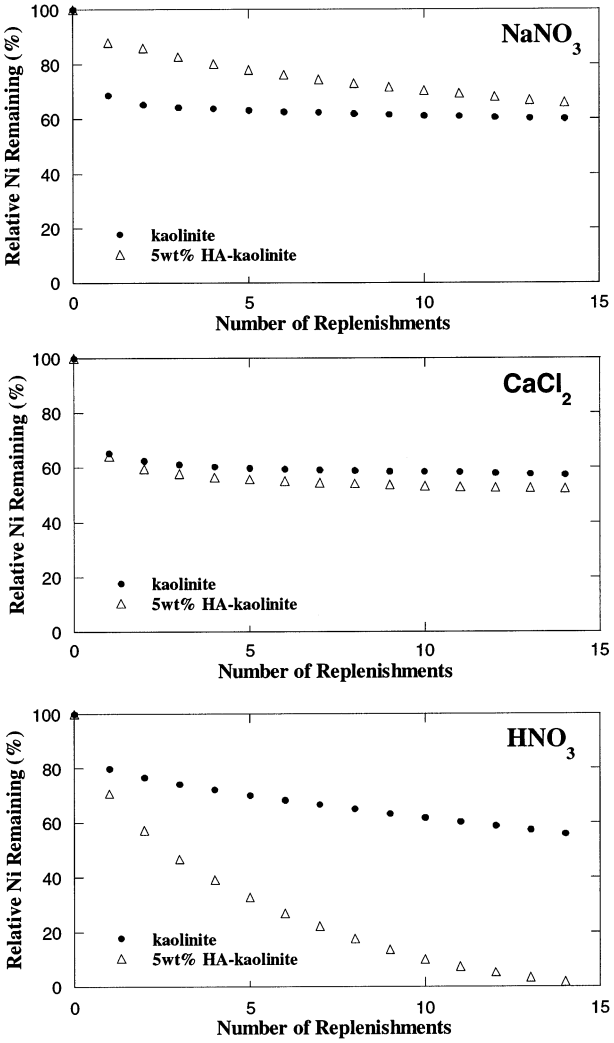

FIGURE 2. Percentage Ni remaining at the kaolinite or the 5 wt % HA-kaolinite surface after desorption with (A) the background electrolyte (pH 7.5, $I = 0.02$ M $NaNO_3$), (B) a calcium chloride solution (pH 6.0, $I = 0.1$ M $CaCl_2$), or (C) a nitric acid solution (pH 4.0).

kaolinite−HA coating−water interfaces, desorption experiments were carried out. Three desorption agents were employed: a background electrolyte solution (pH 6.0, $I =$ 0.02 M), a calcium chloride solution pH 6.0, $I = 0.1$ M), and a nitric acid (pH 4.0) solution. The background solution is most likely to remove any weakly held outer-sphere complexes. The calcium solution, which is 2 orders higher in concentration than the nickel solution, can out-compete Ni at HA binding sites where electrostatic interactions dominate (*39, 40*) and is expected to remove most electrostatically bound Ni from the HA. Nitric acid can remove Ni from both the HA, by proton competition, and from a precipitate phase by proton dissolution. Proton dissolution is especially effective when a less stable nickel hydroxide is being formed (*41*).

The relative amount of Ni remaining on the surface is plotted versus the number of replenishments (Figure 2). Nickel desorption behavior from the kaolinite surface changed little as the number of desorption replenishments is increased. Only HNO_3 slowly released Ni with each replenishment. The initial 30% Ni released from the kaolinite sample with the first replenishment included some Ni entrapped in the wet paste after centrifugation and weak, electrostatically bound Ni. The remaining 70% could not be desorbed from the kaolinite surface with the $CaCl_2$ or the $NaNO_3$ background solutions. Similar results for desorption

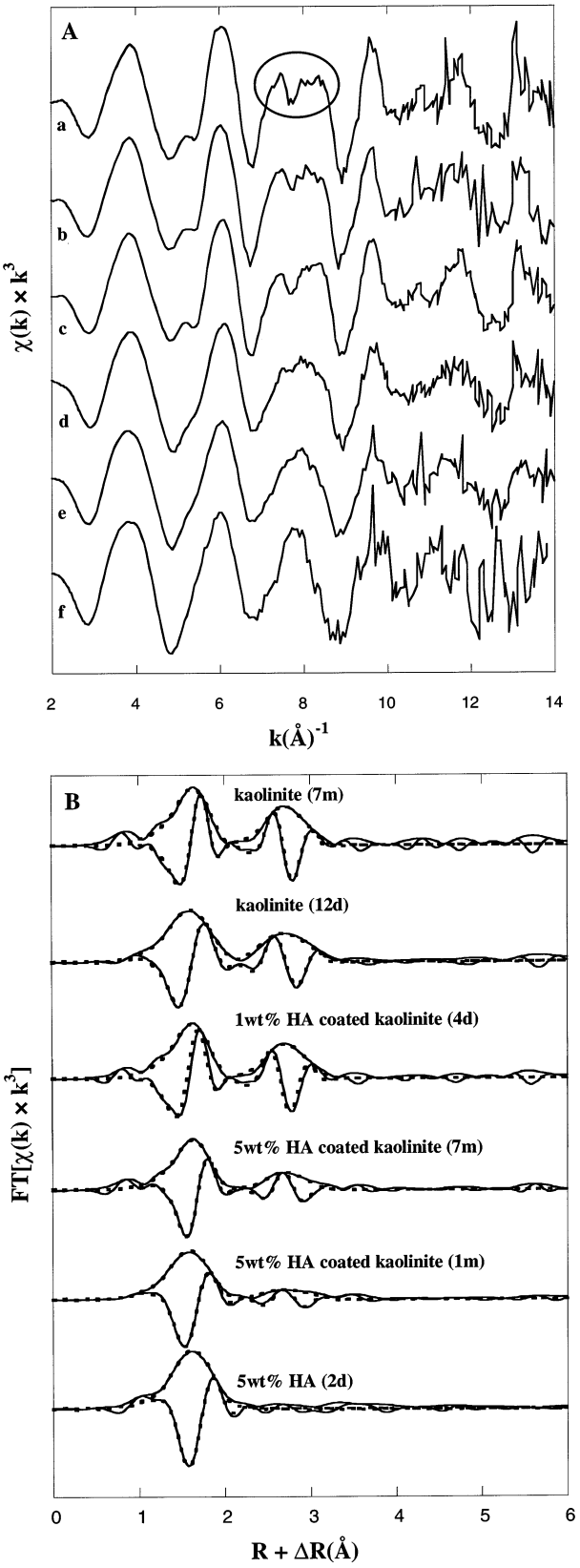

FIGURE 3. Ni Kα EXAFS spectra of kaolinite reacted with Ni for 7 months (a) and 12 days (b), 1 wt % HA-coated kaolinite reacted with Ni for 4 days (c), 5 wt % HA-coated kaolinite reacted with Ni for 7 months (d) and 27 days (e), and HA reacted with Ni for 2 days (f). The k^3-weighted χ functions are shown in panel A. The Fourier transforms of the XAS spectra are shown (uncorrected for phase shifts) in panel B, with solid lines indicating the magnitude and imaginary part and the dotted symbols the best fits.

TABLE 2. Best-Fit Structural Parameters Derived from EXAFS Analysis[a]

		Ni−O			Ni−Ni/C/Al					
	rt	CN	R (Å)	σ^2 (Å^2)	atom	CN	R (Å)	σ^2 (Å^2)	ΔE_0 (eV)	% res
Single Components										
HA	48 h	6.0	2.06	0.004					−1.93	2.52
HA	48 h	5.8	2.05	0.005	C	1.8	2.85	0.010	−2.93	2.13
kaolinite	12 d	6.3	2.05	0.006	Ni	3.2	3.06	0.007	−2.04	5.44
kaolinite	7 m	5.9	2.04	0.005	Ni	4.0	3.06	0.006	−2.06	6.63
kaolinite	7 m	5.4	2.04	0.004	Ni	3.5	3.06	0.007	−2.81	
					Al	3.2	3.20	0.020	−2.81	4.82
Coated Samples										
1 wt % HA-kaolinite	4d	5.2	2.04	0.005	Ni	3.0	3.05	0.006	−2.26	12.91
5 wt % HA-kaolinite	27d	5.5	2.04	0.005	Ni	1.4	3.06	0.005	−2.75	8.63
5 wt % HA-kaolinite	7m	5.7	2.04	0.006	Ni	1.9	3.06	0.006	−1.81	20.30
References (*13*)										
α-nickel hydroxide		5.5	2.04	0.005	Ni	5.6	3.09	0.006		
LDH Ni/Al = 1.3		5.4	2.05	0.004	Ni	2.8	3.06	0.004		

[a] rt, reaction time. CN, coordination number (±20%; *44*). R, interatomic distance (±0.02 Å; *44*). σ^2 (Å^2), Debye−Waller factor. ΔE_0, phase shift. % res, residual error.

of Ni, after 6 months of contact time with mineral surfaces, were observed by others (*41*, *14*). The presence of this resistant fraction has been attributed to the formation and subsequent stabilization of a surface precipitate.

Nickel desorption form HA-coated kaolinite was markedly different than what was observed for the pristine kaolinite system. The $CaCl_2$ solution was more effective in removing a small nickel fraction than the $NaNO_3$ solution, suggesting that a small Ni portion (∼35%) is bound directly to the HA. However, a stable Ni fraction (∼65%) could not be desorbed by either the $CaCl_2$ or the $NaNO_3$ background solution. The HNO_3 solution desorbed essentially all Ni from the HA-coated kaolinite samples with 14 replenishments. This slow, yet total Ni release has been found to be characteristic of Ni release from nickel hydroxide phases, which are not stable to proton dissolution (*41*).

From the sorption and desorption studies, it may be concluded that the HA coating almost tripled the total Ni uptake, but the sorption complex formed in the presence of this coating is less stable to proton-promoted dissolution than the sorption complex formed in the absence of the coating.

EXAFS Spectroscopy. The structure of the dominant Ni sorption complex formed at the different solid−water interfaces can be inferred from EXAFS analysis. Figure 3A shows the background-subtracted k^3 weighted χ functions of the Ni-reacted kaolinite, HA, and kaolinite coated with 1 and 5 wt % HA. The Fourier-transformed radial structure functions (RSF), which are uncorrected for phase shifts, are plotted in Figure 3B. The solid lines represent the magnitude and imaginary part, and the dotted lines represent the best fits resulting from multiple shell fitting. The first peak in the RSF at ∼1.8 Å is indicative of backscattering from the first ligand shell, and the second peak at ∼2.8 Å indicates backscattering from the first metal shell. This metal shell could be fit with Ni in the case of the 12 days reacted kaolinite and the HA-coated kaolinite samples and a combination of Ni and Al in the 7 months reacted kaolinite. The Ni−Ni/Al peak increases in intensity over time in both the kaolinite and the coated kaolinite systems. This increase in intensity of the second shell qualitatively indicates the growth of a Ni-containing precipitate phase.

In Table 2, the structural parameters derived from EXAFS analysis are shown. The coordination number (CN) of the Ni−O shell is approximately equal to six for all samples, indicating that Ni is in an octahedral environment in all sorption complexes. The Ni−O bond distance is the same in all samples, except for the HA sample where the Ni−O bond distance is slightly higher and closer to Ni−O bond distances of Ni in aqueous solutions (*42*). The Ni−Ni bond distances of the surface precipitates are around 3.06 Å, which are significantly shorter than that of a pure Ni hydroxide phase (β-$NiOH_2$), 3.12 Å, and of a nickel hydroxide with 50% vacancies in the octahedral layer (α- $NiOH_2$), 3.09 Å (Table 2). This contraction in bond length has been attributed to several factors, including the presence of both Al and Ni in the octahedral layers where the smaller Al atom forces the Ni−Ni bond length to contract (*15*). The low Ni−Ni coordination number in the 5 wt % HA−kaolinite mixtures indicates that in these samples the development of a surface precipitate phase is still in an initial phase after 7 months.

The presence of a high-frequency beat in the Ni−HA χ function (Figure 3A) indicates the presence of higher order shells. A small Fourier peak around ∼2.3 Å could only be fit with a Ni−C scattering path at 2.85 Å and with a CN of ∼1.8 (Table 2). Xia et al. (*43*) found similar results for a Ni-reacted HA, with two carbon atoms at an average radial distance of 2.93 Å. These results indicate that, under the reaction conditions applied, Ni forms a bidentate inner-sphere complex with carbon-containing functional groups of HA. Carboxylic and phenolic functional groups are the most likely candidates to bond with Ni because of their abundance and reactivity at the pH employed (*19*). However, weak backscattering contributions from low Z elements beyond the first shell prevent a more detailed analysis (*28*). The absence of a Ni−Ni shell in the Ni-reacted HA sample confirms that these systems were not supersaturated with respect to bulk precipitation of a nickel hydroxide/carbonate phase under the reaction conditions of this study.

The precipitate formed at the kaolinite surface after 12 days of reaction contains three Ni atoms at an average radial distance of 3.06 Å. After 7 months of reaction, the precipitate contains 3 Ni atoms at 3.06 Å and ∼3 Al atoms at 3.20 Å. Similar results have been found for Co- (*11*, *12*) and Ni-containing (*4*, *31*) precipitates formed at the kaolinite surface and indicate that the initial nickel hydroxide transforms into a more stable mixed Ni−Al layered double hydroxide (LDH) over time. The fit for the 7-month reacted kaolinite significantly improved when an Al path was included in the fit (Table 2), suggesting the presence of both Ni and Al in the octahedral layer of the precipitate phase. No meaningful fits were obtained in other samples when Al was included. Because of similar Ni−Ni and Ni−Al bond distances in Ni−Al LDH and the weak backscattering of Al compared to Ni, this inability to fit Al in the octahedral layer is not necessarily a proof of the absence of Al in the octahedral layer. Infor-

mation on the presence of Al in the precipitate can be obtained from the χ functions (Figure 3A). A characteristic beat pattern at 8−9 $Å^{-1}$ has been found by Scheinost and Sparks to be solely produced by the presence of second shell Al (*15*). This characteristic beat pattern is present in the kaolinite and the kaolinite coated with 1 wt % HA samples, indicating the formation of a mixed Ni−Al LDH in these samples. The absence of this characteristic beat pattern in the 5 wt % HA-coated kaolinite spectra indicates that the precipitate formed is a $NiOH_2$ phase rather than a mixed LDH. These results complement the desorption studies and show that a stable Ni−Al LDH is formed at the kaolinite surface and at the kaolinite surface in the presence of a 1 wt % organic coating, while a less stable (with respect to proton dissolution) nickel hydroxide is being formed in the presence of a 5 wt % organic coating.

The goodness of the fit (% residual in Table 2) is not as good for the coated samples as for the individual components. This indicates that, apart from a nickel-containing precipitate, another nickel sorption complex is present, which dilutes the EXAFS signal from the precipitate phase. The dissolution studies indicated that about 40% of the nickel is bound to the HA, whereas 60% is included in a precipitate phase. Therefore, the dilution of the EXAFS signal from the Ni−Ni shell by a Ni−C path is expected, but this Ni−C path could not be fit. This is not very surprising since low Z elements hardly contribute to the EXAFS signal.

This research shows that a Ni-containing precipitate phase is formed at the kaolinite surface, even in the presence of a 5 wt % organic coating. Ni uptake kinetics and capacity increases with the amount of HA coated at the kaolinite surface, but the formation of a surface precipitate is slowed significantly with a higher amount of HA coating. The precipitate formed in the presence of a 5 wt % HA coating is nickel hydroxide, whereas in the presence of a 1 wt % HA coating a more stable Ni−Al LDH is formed. Both precipitates are resistant to desorption with mild desorption agents, but the nickel hydroxide precipitate is not stable with respect to proton dissolution. These results should be included in any complexation model and may be of value in developing sound remediation strategies for soils contaminated with toxic first row transition metals.

Acknowledgments

This research was funded by the USDA-NRICGP. The authors thank Drs. Davies and Ghabbour (Northeastern University, Boston, NH) for kindly providing the humic acid used in this study and Kaumudi Pandya (Brookhaven National Laboratory, Upton, NY) for her support during the XAFS measurements. Thanks are also extended to M. Gräfe and Drs. D. Peak and P. Trivedi for their critical comments on the manuscript.

Literature Cited

(1) Hochella, M. F. In *Mineral−Water Interface Geochemistry*; Hochella, M. F., Jr., White, A. F., Eds.; Mineralogical Society of America: Washington, DC, 1990; Vol. 23, pp 87−132.
(2) Sparks, D. L. *Environmental Soil Chemistry*; Academic Press: London, 1995.
(3) Fendorf, S. E.; Lamble, G. M.; Stapleton, M. G.; Kelley, M. J.; Sparks, D. L. *Environ. Sci. Technol.* **1994**, *28*, 284−289.
(4) Scheidegger, A. M.; Lamble, G. M.; Sparks, D. L. *J. Colloid Interface Sci.* **1997**, *186*, 118−128.
(5) O'Day, P. A.; Brown, G. E., Jr.; Parks, G. A. *J. Colloid Interface Sci.* **1994**, *165*, 269−289.
(6) Towle, S. N.; Bargar, J. R.; Brown, G. E., Jr.; Parks, G. A. *J. Colloid Interface Sci.* **1997**, *187*, 62−82.
(7) Xia, K.; Mehadi, A.; Taylor, R. W.; Bleam, W. F. *J. Colloid Interface Sci.* **1997**, *185*, 252−257.
(8) Cheah, S. F.; Brown, G. E., Jr.; Parks, G. A. *J. Colloid Interface Sci.* **1998**, *208*, 110−128.
(9) Schlegel, M. L.; Charlet, L.; Manceau, A. *J. Colloid Interface Sci.* **1999**, *220*, 392−405.
(10) Ford, R. G.; Sparks, D. L. *Environ. Sci. Technol.* **2000**, *34*, 2479−2483.
(11) Thompson, H. A.; Parks, G. A.; Brown, G. E., Jr. *Clays Clay Miner.* **1999**, *47*, 425−438.
(12) Thompson, H. A.; Parks, G. A.; Brown, G. E., Jr. *Geochim. Cosmochim. Acta* **1999**, *63*, 1767−1779.
(13) Manceau, A.; Schlegel, M.; Nagy, K. L.; Charlet, L. *J. Colloid Interface Sci.* **1999**, *220*, 181−197.
(14) Ford, R. G.; Scheinost, A. C.; Scheckel, K. G.; Sparks, D. L. *Environ. Sci. Technol.* **1999**, *33*, 3140−3144.
(15) Scheinost, A. C.; Sparks, D. L. *J. Colloid Interface Sci.* **2000**, *223*, 167−178.
(16) Scheckel, K. G.; Scheinost, A. C.; Ford, R. G.; Sparks, D. L. *Geochim. Cosmochim. Acta* **2000**, *64*, 2727−2735.
(17) Morin, G.; Ostergren, J. D.; Juillot, F.; Ildefonse, P.; Calas, G.; Brown, G. E., Jr. *Am. Mineral.* **1999**, *84*, 420−434.
(18) Manceau, A.; Lanson, B.; Schlegel, M. L.; Hargré, J. C.; Musso, M.; Eybert-Bérard, L.; Hazemann, J.-L.; Chateigner, D.; Lamble, G. M. *Am. J. Sci.* **2000**, *300*, 289−343.
(19) Stevenson, F. J. *Humus Chemistry. Genesis, Composition, Reactions*, 2nd ed.; Wiley & Sons: New York, 1994.
(20) Vermeer, A. W. P.; McCulloch, J. K.; Van Riemsdijk, W. H.; Koopal, L. K. *Environ. Sci. Technol.* **1999**, *33*, 3892−3897.
(21) Pétrović, M.; Kaštelan-Macan, M.; Horvat, A. J. M. *Water Air, Soil Pollut.* **1999**, *111*, 41−56.
(22) Roberts, D. R.; Scheidegger, A.; Sparks, D. *Environ. Sci. Technol.* **1999**, *33*, 3749−3754.
(23) Elzinga, E. J.; Sparks, D. L. *J. Colloid Interface Sci.* **1999**, *213*, 506−512.
(24) Yamaguchi, N. U.; Scheinost, A. C.; Sparks, D. L. *Soil Sci. Soc. Am. J.* **2001**, *65*, 729−736.
(25) Zachara, J. M.; Resch, C. T.; Smith, S. C. *Geochim. Cosmochim. Acta* **1994**, *58*, 553−556.
(26) Templeton, A. S.; Trainor, T. P.; Traina, S. J.; Spormann, A. M.; Brown, G. E., Jr. *Proc. Natl. Acad. Sci. U.S.A.* **2001**, *98*, 11897−11902.
(27) Jackson, M. L. *Soil Chemical Analysis−Advanced Course*; University of Wisconsin: Madison, WI, 1956.
(28) Davies, G.; Fataftah, A.; Cherkasskly, A.; Ghabbour, E. A.; Radwan, A.; Jansen, S. A.; Kolla, S.; Paciolla, M. D.; Sein, L. T., Jr.; Buermann, W.; Balasubramanian, M.; Budnick, J.; Xing, B. *J. Chem. Soc., Dalton Trans.* **1997**, 4047−4060.
(29) Mattigod, S. V.; Rai, D.; Felmy, A., R.; Rao, L. *J. Solution Chem.* **1997**, *26*, 391−403.
(30) Eick, M. J.; Fendorf, S. E. *Soil Sci. Soc. Am. J.* **1998**, *62*, 1257−1267.
(31) Mellini, M. *Am. Mineral.* **1982**, *67*, 587−598.
(32) Pennell, K. D.; Boyd, S. A.; Abriola, L. M. *Soil Sci. Soc. Am. J.* **1995**, *59*, 1012−1018.
(33) deJonge, H.; Mittelmeijer-Hazeleger, M. C. *Environ. Sci. Technol.* **1996**, *30*, 408−413.
(34) Ghabbour, E. A.; Davies, G.; O'Donaughy, K.; Smith, T. L.; Goodwillie, M. E. In *Humic Substances. Structures, Properties and Uses*; Davies, G., Ghabbour, E. A., Eds.; The Royal Society of Chemistry: Cambridge, 1998; p 259.
(35) Benjamin, M. M.; Leckie, J. O. *J. Colloid Interface Sci.* **1981**, *79*, 209−221.
(36) Papelis, C. *Environ. Sci. Technol.* **1995**, *29*, 1526−1533.
(37) Strawn, D. G.; Sparks, D. L. *Soil Sci. Soc. Am. J.* **2000**, *64*, 144−156.
(38) Axe, L.; Trivedi, P. *J. Colloid Interface Sci.* **2002**, *247*, 259−265.
(39) Naylor, D. V.; Overstreet, R. *Soil Sci. Soc. Am. J.* **1969**, *33*, 848−851.
(40) Mandal, R.; Salam, M. S. A.; Murimboh, J.; Hassan, N. M.; Chakrabarti, C. L.; Back, M. H.; Grégoire, D. C. *Environ. Sci. Technol.* **2000**, *34*, 2201−2208.
(41) Scheckel, K. G.; Sparks, D. L. *Soil Sci. Soc. Am. J.* **2001**, *65*, 685−694.
(42) Pandya, K. I.; O'Grady, W. E.; Corrigan, D. A.; McBreen, J.; Hoffman, R. W. *J. Phys. Chem.* **1990**, *94*, 21−26
(43) Xia, K.; Bleam, W.; Helmke, P. A. *Geochim. Cosmochim. Acta* **1997**, *61*, 2223−2235.
(44) O'Day, P. A.; Rehr, J. J.; Zabinsky, S. I.; Brown, G. E. J. *J. Am. Chem. Soc.* **1994**, *116*, 2938−2949.

Received for review May 17, 2002. Revised manuscript received November 5, 2002. Accepted November 13, 2002.

ES025803W